© 2017. Published by The Company of Biologists Ltd | Development (2017) 144, 3303-3314 doi:10.1242/dev.154013

RESEARCH ARTICLE

# Dnmt1-dependent Chk1 pathway suppression is protective against neuron division

**Mio Oshikawa[1], Kei Okada[1], Hidenori Tabata[2], Koh-ichi Nagata[2] and Itsuki Ajioka[1,3,*]**


## ABSTRACT

Neuronal differentiation and cell-cycle exit are tightly coordinated, even in pathological situations. When pathological neurons re-enter the cell cycle and progress through the S phase, they undergo cell death instead of division. However, the mechanisms underlying mitotic resistance are mostly unknown. Here, we have found that acute inactivation of retinoblastoma (Rb) family proteins (Rb, p107 and p130) in mouse postmitotic neurons leads to cell death after S-phase progression. Checkpoint kinase 1 (Chk1) pathway activation during the S phase prevented the cell death, and allowed the division of cortical neurons that had undergone acute Rb family inactivation, oxygen-glucose deprivation (OGD) or *in vivo* hypoxia-ischemia. During neurogenesis, cortical neurons became protected from S-phase Chk1 pathway activation by the DNA methyltransferase Dnmt1, and underwent cell death after S-phase progression. Our results indicate that Chk1 pathway activation overrides mitotic safeguards and uncouples neuronal differentiation from mitotic resistance.


**KEY WORDS: Cell cycle, Cerebral cortical neurons, Stroke, Chk1, Dnmt1, Retinoblastoma proteins**

## INTRODUCTION

One of the fundamental concepts in neurobiology and neuropathology is that differentiated neurons cease to divide. During development, neural stem/progenitor daughter cells exit the cell cycle and enter the postmitotic G0 phase to undergo neuronal differentiation (Ajioka, 2014; Dyer and Cepko, 2001; Edlund and Jessell, 1999; Guillemot et al., 2006). The postmitotic feature of differentiating neurons is believed to be irreversible, because the regulatory networks that promote cell cycling are incompatible with those that direct and maintain neuronal differentiation. In the cerebral cortex, apical progenitors (radial glia cells) and basal progenitors (intermediate progenitor cells) differentiate into excitatory neurons that immediately undergo a postmitotic transition (Dehay and Kennedy, 2007; Kriegstein and Alvarez-Buylla, 2009). Although various progenitor cells continue to be uncovered (Florio and Huttner, 2014), the seminal studies to determine the birthdate of a neuron reinforce the concept that differentiating neurons undergo a postmitotic transition immediately after exiting the cell cycle (Angevine and Sidman, 1961; Sidman et al., 1959).

The tight coordination of cell-cycle exit and neuronal differentiation contributes not only to the precise regulation of neuronal development, but also to the progression of neuronal disorders (Heintz, 1993; Herrup and Yang, 2007). In pathological situations, postmitotic neurons re-enter the cell cycle, but then undergo cell death instead of division. For example, in Alzheimer's disease (AD), Parkinson's disease (PD) and a mouse model for stroke, neurons enter the S phase and then undergo cell death (El-Khodor et al., 2003; Hoglinger et al., 2007; Kuan et al., 2004; Yang et al., 2001). As inhibiting cell-cycle re-entry prevents pathological neuron death (Osuga et al., 2000), cell-cycle re-entry is thought to contribute to disease progression.

The retinoblastoma protein family [Rb (Rbl), p107 (Rbl1) and p130 (Rbl2)] plays a central role in preventing cells from entering the S phase (Burkhart and Sage, 2008; Weinberg, 1995). During G1 to S-phase progression, the phosphorylation of Rb family proteins leads to their dissociation from E2F transcription factors, resulting in S-phase-related gene expression. Rb phosphorylation is also correlated with the cell-cycle re-entry of pathological neurons (Nguyen et al., 2003; Yu et al., 2012) and the progression of AD (Biswas et al., 2007; Silva et al., 2014).

In addition to regulating S-phase entrance, the Rb family coordinates cell-cycle exit and neuronal differentiation. When Rb family expression is lost in neuronal progenitor cells, the subsequent coordination of cell-cycle exit and neuronal differentiation is lost, and differentiated neurons can divide in some cases. For example, *p107*-single mouse retinal progenitors, which lack Rb family members except for one *p107* allele ($Rb^{-/-}$; $p107^{+/-}$; $p130^{-/-}$), differentiate into mature horizontal interneurons that proliferate and form tumors (Ajioka et al., 2007). Differentiating mouse amacrine-like cells and human cone photoreceptor cells also proliferate and form tumors when retinal progenitors are deficient in mouse *Rb* and *p107* or human *RB1*, respectively (Chen et al., 2004; Xu et al., 2014). In the mouse cerebral cortex, loss of the Rb family or of just *Rb* in cortical progenitors results in immature neurons that undergo cell division (Ferguson et al., 2002; Lee et al., 1994; MacPherson et al., 2003; Oshikawa et al., 2013). However, the induction of Rb family loss in postmitotic neurons immediately after cell-cycle exit does not result in cell division, even though they enter the S phase (Oshikawa et al., 2013). Thus, once progenitor daughter cells exit the cell cycle and initiate neuronal differentiation, they are prevented from undergoing cell division and maintain mitotic resistance even after acute Rb family inactivation. These findings led us to hypothesize that pathological neurons in the S phase undergo cell death by activating mitotic safeguards.

Checkpoint kinase 1 (Chk1) contributes to G2/M cell-cycle arrest induced by acute DNA damage stimulation, such as UV exposure (Bartek and Lukas, 2003). On the other hand, in the absence of exogenic DNA damage, Chk1 is essential for the survival and

[1]Center for Brain Integration Research (CBIR), Tokyo Medical and Dental University (TMDU), Tokyo 113-8510, Japan. [2]Department of Molecular Neurobiology, Institute for Developmental Research, Aichi Human Service Center, Kasugai Aichi 480-0392, Japan. [3]The Japan Science and Technology Agency (JST), Precursory Research for Embryonic Science and Technology (PRESTO), 4-1-8 Honcho, Kawaguchi, Saitama 332-0012, Japan.

*Author for correspondence (iajioka@ams.kuramae.ne.jp)

K.N., 0000-0002-6827-8434; I.A., 0000-0001-9997-1525

**Received 30 April 2017; Accepted 1 August 2017**

Development (2017) 144, 3303-3314 doi:10.1242/dev.154013

proliferation of mouse embryonic stem cells (ESCs) and mouse embryonic fibroblasts (MEFs) (Liu et al., 2000; Naruyama et al., 2008; Shimada et al., 2008; Takai et al., 2000). In neuroblastoma cells, Chk1 inhibition during the S phase causes cell death (Cole et al., 2011), suggesting the possibility that Chk1 pathway activation in the S phase inactivates mitotic safeguards and promotes subsequent cell division even in other cell types.

In this study, we have found that the Chk1 pathway was activated during the S phase in proliferative cortical neurons generated from mouse Rb triple knockout (Rb-TKO, *Rb*$^{-/-}$*; p107*$^{-/-}$*; p130*$^{-/-}$) progenitors, but not in non-proliferative cortical neurons after acute Rb family inactivation. Chk1 pathway activation was essential for the survival of neurons generated from Rb-TKO progenitors, and was sufficient for the division of neurons that have undergone acute Rb family inactivation. Notably, Chk1 pathway activation prevented oxygen-glucose-deprived (OGD) cortical neurons in the S phase from undergoing cell death and allowed them to divide. These results indicate that Chk1 pathway activation prevents cell death and overrides the mitotic resistance of pathological hypoxic neurons and differentiating neurons that have undergone acute Rb family inactivation.

## RESULTS

### Cell death of MAP2-Rb-TKO neurons after S-phase progression

To develop a pathological model in which postmitotic neurons undergo cell death after S-phase progression, we used an Rb family triple knockout model. We recently developed a technique for conditionally inactivating all of the Rb family members in postmitotic immature neurons immediately after cell-cycle exit, by *ex vivo* electroporation with Cre-expressing plasmids containing a neuron-specific pMAP2 promoter. We visualized the Rb-TKO cells using a GFP-Cre reporter. Using this technique, we found that pMAP2-induced Rb-TKO (MAP2-Rb-TKO) cells progressed through the S phase, while one allele of *Rb* (Rb-single; *Rb*$^{+/-}$*; p107*$^{-/-}$*; p130*$^{-/-}$) was sufficient to prevent S-phase entry (Oshikawa et al., 2013). We have previously reported that pMAP2-Cre activated in the ventricular/subventricular zone (VZ/SVZ) and preferentially labeled postmitotic immature neurons immediately after cell-cycle exit (Oshikawa et al., 2013). These immature neurons in the VZ/SVZ are negative for the basal progenitor marker Tbr2 (Fig. S1A). Immunostaining for the postmitotic neuronal markers doublecortin (DCX) and Satb2 confirmed that postmitotic immature neurons did not de-differentiate after acute Rb family inactivation (Fig. S1B-E). As neurons die after S-phase progression in pathological situations, we examined whether the MAP2-Rb-TKO immature neurons in the S phase undergo cell death. We labeled the cells with 5-ethynyl-2'-deoxyuridine (EdU) for 24 h before fixation, and then immunostained them for the cell-death marker activated caspase 3 (AC3) (Fig. 1A). We scored the cells using stereology, which is a method that uses random and systematic sampling to yield unbiased and quantitative data (West et al., 1991). We randomly counted the cryosections of explant tissues and the dissociated cells on slides as described in the figure legends and the Materials and Methods. The percentages of total AC3-positive cells and AC3/EdU double-positive cells were significantly higher in MAP2-Rb-TKO cultures than in control MAP2-Rb-single cultures (Fig. 1B-D). To exclude the possibility that the AC3-positive cells had undergone DNA repair and incorporated EdU, we measured their DNA content by 4′,6-diamidino-2-phenylindole (DAPI) staining, and found that 14.21±5.36% of the MAP2-Rb-TKO cells in the G2/M phase were AC3 positive (Fig. 1E-H). To confirm that the cell death following S-phase progression was not an artifact of the explant cultures, we performed EdU labeling at 4 days *in utero* (DIU) and found that some of the EdU-positive cells at 5 DIU were also AC3 positive (Fig. S1F,G). These results suggested that MAP2-Rb-TKO immature neurons in the S phase underwent cell death instead of dividing.

### An essential role for Chk1 in Rb-TKO neuron survival and division

When the Rb family is inactivated using pCAG-Cre in which Cre is expressed from a ubiquitous promoter, immature neurons generated from the pCAG-induced Rb-TKO (CAG-Rb-TKO) progenitors divide (Oshikawa et al., 2013). Immunostaining for DCX, Satb2 and the apical progenitor marker nestin confirmed that the CAG-Rb-TKO cells initiated neuronal differentiation similar to the Rb-single control cells (Fig. S2A-F). However, in contrast to the Satb2-positive control cells, 13.9±1.2% and 2.02±0.06% of the Satb2-positive CAG-Rb-TKO cells were immunopositive for EdU and phospho-histone H3 (pH3), respectively (Fig. 2A,B, Fig. S2G,H), suggesting that the CAG-Rb-TKO progenitor cells initiated neuronal differentiation without cell-cycle exit and underwent cell division. Of the nestin-positive wild-type cells, 1.90±0.34% were pH3 positive, (Fig. S2I,J), suggesting that the Satb2-positive CAG-Rb-TKO immature neurons were highly proliferative, similar to the wild-type progenitor cells. To determine the fate of CAG-Rb-TKO neurons after the mitotic phase, we performed 5-bromo-2′-deoxyuridine (BrdU)-labeling at 4 days in culture (DIC) for 1 h and EdU labeling at 5 DIC (Fig. S3A). In the CAG-Rb-TKO culture, most of the BrdU-positive cells detected at 4 DIC were still detected at 5 DIC (Fig. S3B,C), and 6.4% of the cells were also EdU positive (Fig. S3D), suggesting that CAG-Rb-TKO neurons continued to cycle after cell division. We also confirmed that it was not an artifact of the explant cultures using *in utero* electroporation analysis (Fig. S3E-G).

To examine the mechanism underlying the different fates of the CAG- and MAP2-Rb-TKO cells after S-phase progression, we focused on the Chk1 and Chk2 pathways, as we have previously found that a DNA repair pathway contributes to CAG-Rb-TKO cell division (Oshikawa et al., 2013). At 4 DIC, the proportion of cells that were immunopositive for phospho-Chk1 (pChk1, Ser317) and phospho-Chk2 (pChk2, Thr68) was significantly increased in the CAG-Rb-TKO cells compared with the CAG-Rb-single control cells (Fig. 2C-F) and the MAP2-Rb-TKO cells (Fig. S2K,L). To determine the cell-cycle phase of the pChk1-, and pChk2-positive CAG-Rb-TKO cells, we performed EdU labeling for 1 h before fixation. More than 85% of each cell population was positive for the cortical neuron marker Satb2 (Fig. 2G-I), and more than 70% was EdU positive (Fig. 2J-L), suggesting that the Chk1 and Chk2 pathways were activated during S phase in CAG-Rb-TKO immature neurons.

To determine the role of the Chk1 and Chk2 pathways in the division of CAG-Rb-TKO immature neurons, we treated the cells with Chk1/Wee1, Wee1 and Chk2 inhibitors for 16 h before fixation. These inhibitors did not reduce the proportion of EdU-positive cells (Fig. S4A), but the Chk1/Wee1 inhibitor suppressed the increase in cells that were double-positive for pH3 and Satb2 (Fig. 3A). To determine the involvement of kinases upstream of Chk1/2, we treated the cells with inhibitors of the ataxia telangiectasia and Rad3-related protein (ATR) and ataxia telangiectasia mutated (ATM) pathways. Only the ATR/ATM inhibitor suppressed the increase in pH3/Satb2 double-positive cells

Development (2017) 144, 3303-3314 doi:10.1242/dev.154013

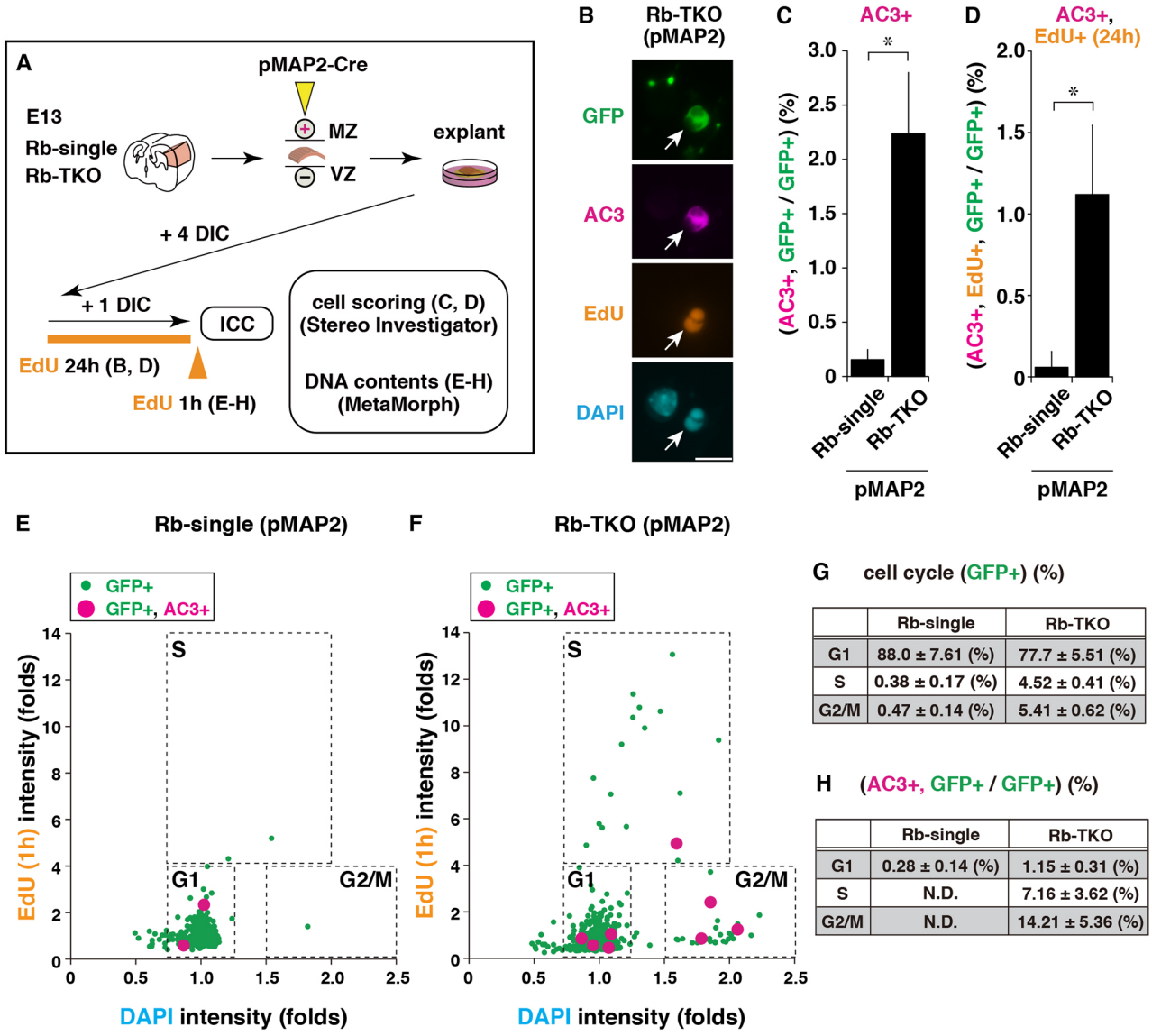


**G** cell cycle (GFP+) (%)

| | Rb-single | Rb-TKO |
|---|---|---|
| G1 | 88.0 ± 7.61 (%) | 77.7 ± 5.51 (%) |
| S | 0.38 ± 0.17 (%) | 4.52 ± 0.41 (%) |
| G2/M | 0.47 ± 0.14 (%) | 5.41 ± 0.62 (%) |

**H** (AC3+, GFP+ / GFP+) (%)

| | Rb-single | Rb-TKO |
|---|---|---|
| G1 | 0.28 ± 0.14 (%) | 1.15 ± 0.31 (%) |
| S | N.D. | 7.16 ± 3.62 (%) |
| G2/M | N.D. | 14.21 ± 5.36 (%) |

**Fig. 1. Neuronal cell death after S-phase progression in response to acute Rb family inactivation.** (A) Experimental design: Cre-expressing plasmids were used to inactivate Rb family members in cortical explants from Rb-single (*Z/EG; Rb*$^{Lox/+}$*; p107*$^{-/-}$*; p130*$^{Lox/Lox}$) and Rb-TKO (*Z/EG; Rb*$^{Lox/Lox}$*; p107*$^{-/-}$*; p130*$^{Lox/Lox}$) mice. At 5 DIC, the cortical explants were dissociated and plated on chamber slides for immunocytochemistry (ICC). After immunostaining, cell scoring and DNA content analysis were performed. (B) GFP (green), AC3 (magenta) and EdU (orange) immunofluorescence images of MAP2-Rb-TKO cells. Nuclei were visualized using DAPI (cyan). Arrows indicate immunopositive cells. (C,D) Cell scoring of AC3-positive (C) and AC3/EdU double-positive (D) cells. **P*<0.05. (E-H) DNA content analysis of MAP2-Rb-single (E) and MAP2-Rb-TKO (F) cells. Scale bars: 10 µm. VZ, ventricular zone; MZ, marginal zone; N.D., not detected. Data are mean±s.e.m.

(Fig. 3A). The increase in pH3-positive cells was also suppressed by overexpressing Chk1-shRNA (Fig. 3B), which silenced the Chk1 expression (Fig. S4B). This decrease in pH3-positive cells was rescued by overexpressing the shRNA-resistant form of Chk1 (Chk1 SMHA; Fig. 3B). Chk1-shRNA overexpression also reduced the number of BrdU/EdU double-positive cells (Fig. S4C) and increased the proportion of AC3-positive cells (Fig. 3C). Together, these results indicated that Chk1 was essential for the survival and division of the CAG-Rb-TKO immature neurons.

### Chk1 pathway activation is sufficient to induce MAP2-Rb-TKO neuron survival and division

Next, to determine whether Chk1 pathway activation can prevent the MAP2-Rb-TKO immature neuron cell death and induce their division, we used the topoisomerase 1 inhibitor camptothecin (CPT), which activates the Chk1 pathway in the S phase (Cliby et al., 2002). Stimulation with 1 nM CPT increased the proportion of pChk1- and pChk2-positive cells (Fig. 4A,B). In addition, more than 75% of each of these cell populations was also EdU positive (Fig. 4C), suggesting that 1 nM CPT activated the Chk1 pathway during the S phase. Stimulation with 1 nM CPT also increased the proportion of pH3/Satb2 double-positive MAP2-Rb-TKO cells (Fig. 4D), whereas Chk1-shRNA overexpression inhibited this increase (Fig. 4D), suggesting that CPT induced a Chk1-dependent cell division in MAP2-Rb-TKO cells. Stimulation with 1 nM CPT decreased the proportion of AC3-positive cells (Fig. 4E). To demonstrate cell division directly, we performed *in utero* electroporation at E13, prepared cortical slices at E17 and performed time-lapse imaging of MAP2-Rb-TKO cells transfected with H2B-mCherry to visualize the nuclei with and

Development (2017) 144, 3303-3314 doi:10.1242/dev.154013

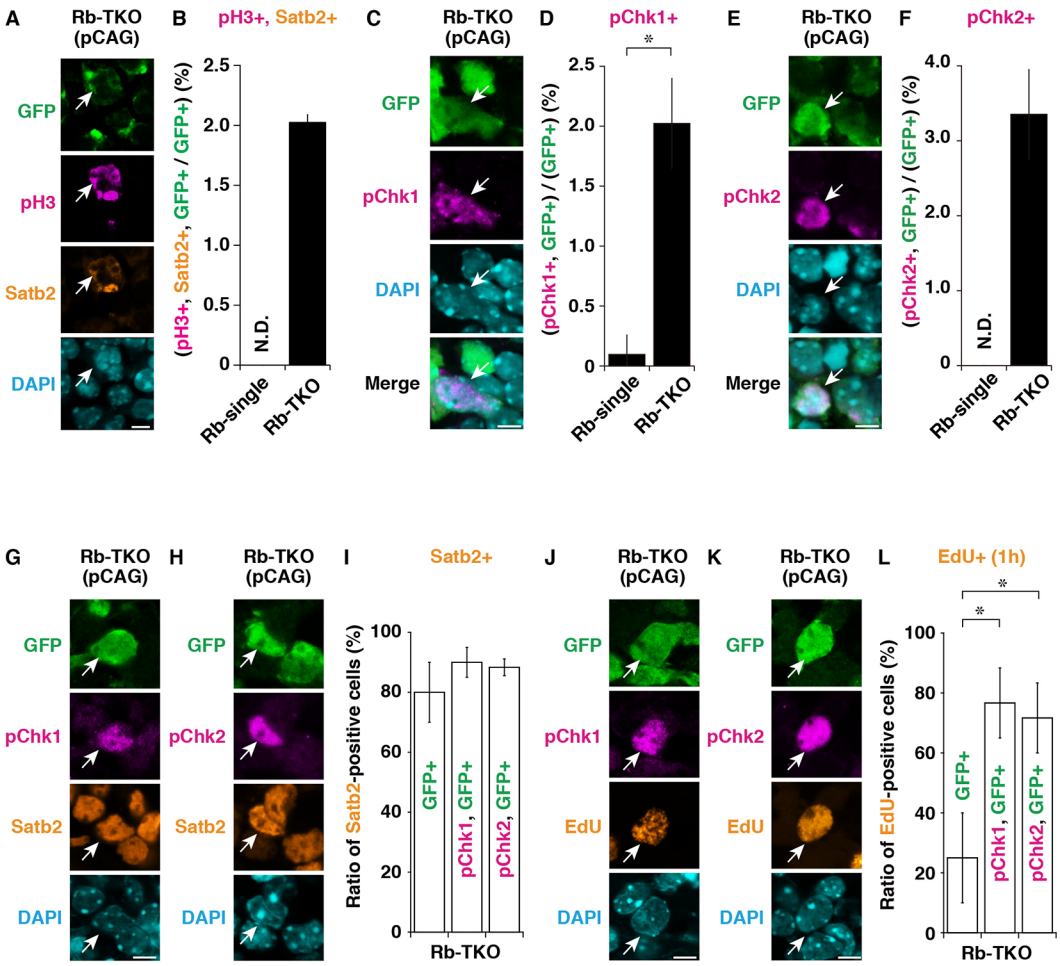


**Fig. 2. Chk1 pathway activation in proliferative CAG-Rb-TKO neurons.** At 4 DIC after the electroporation of Cre-expressing plasmids, cortical explants were fixed, cryosectioned and immunostained. (J-L) The explants were cultured with EdU for 1 h before fixation. (A,C,E,G,H,J,K) GFP (green); pH3 (A), pChk1 (C,G,J) and pChk2 (E,H,K) (magenta); Satb2 (A,G,H) and EdU (J,K) (orange) immunofluorescence images of CAG-Rb-TKO tissues. Nuclei were visualized using DAPI (cyan). Arrows indicate immunopositive cells. (B,D,F,I,L) Cell scoring of immunopositive cells. N.D., not detected. Scale bars: 5 µm. *$P$<0.05. Data are mean±s.e.m.

without 1 nM CPT treatment (Fig. 4F). We have previously reported the migration defect of MAP2-Rb-TKO neurons at postnatal day (P) 2 (Oshikawa et al., 2013). We also found the migration defect was present as early as E17 (Fig. S5A,B,E). However, abnormally migrated MAP2-Rb-TKO cells were both pH3 and AC3 negative at E17 (Fig. S5C,D), suggesting that cell division and cell death by acute Rb family inactivation was not observed by time-lapse imaging analysis. We counted the number of dividing multipolar migrating cells in the intermediate zone (IZ) and confirmed that immature MAP2-Rb-TKO neurons underwent cell division after CPT treatment (Fig. 4F-H, Fig. S5F, Movies 1 and 2). Stimulation with 1 nM CPT also increased the proportion of BrdU/EdU double-positive cells (Fig. S5G).

To determine whether the increase in Chk1 expression is involved in MAP2-Rb-TKO cell division, we examined Chk1 expression level in CAG- and MAP2-Rb-TKO cells. Although Chk1 expression levels were increased after Rb family inactivation, there was no significant difference between CAG- and MAP2-Rb-TKO cells (Fig. S6A). These results suggest that the Chk1 pathway is activated independently of its expression level.

To determine whether the canonical Chk1 pathway that is activated by UV exposure is involved in MAP2-Rb-TKO cell division, we overexpressed a constitutively active form of Chk1 (L449R). Chk1 (L449R) promotes the phosphorylation of Ser345, which is phosphorylated by ATR after UV exposure, and induces the activation of downstream canonical Chk1 pathway (Wang et al., 2012). Overexpressing Chk1 (L449R) in MAP2-Rb-TKO cells inhibited S-phase entry (Fig. S6B), suggesting that canonical Chk1 pathway activation induces cell-cycle arrest rather than cell-cycle progression. If the Chk1 pathway activation that regulates cell division suppressed the canonical Chk1 pathway, Cdc25 phosphatase would be protected from degradation, resulting in the activation of G2/M cyclin-dependent kinase and cell division. We therefore investigated whether Cdc25 overexpression promotes the division of MAP2-Rb-TKO cells. Although overexpressing Cdc25A in MAP2-Rb-TKO cells slightly increased the percentage of EdU-positive cells, as previously reported (Blomberg and Hoffmann, 1999), we did not observe an increased proportion of pH3-positive cells, similar to the result with wild-type Chk1 overexpression (Fig. S6C). These results suggest that the canonical Chk1 pathway is not important for the cell division of MAP2-Rb-TKO immature neurons. In summary, ectopic activation of the non-canonical Chk1 pathway during the S phase allows MAP2-Rb-TKO immature neurons to escape cell death and undergo cell division.

Development (2017) 144, 3303-3314 doi:10.1242/dev.154013

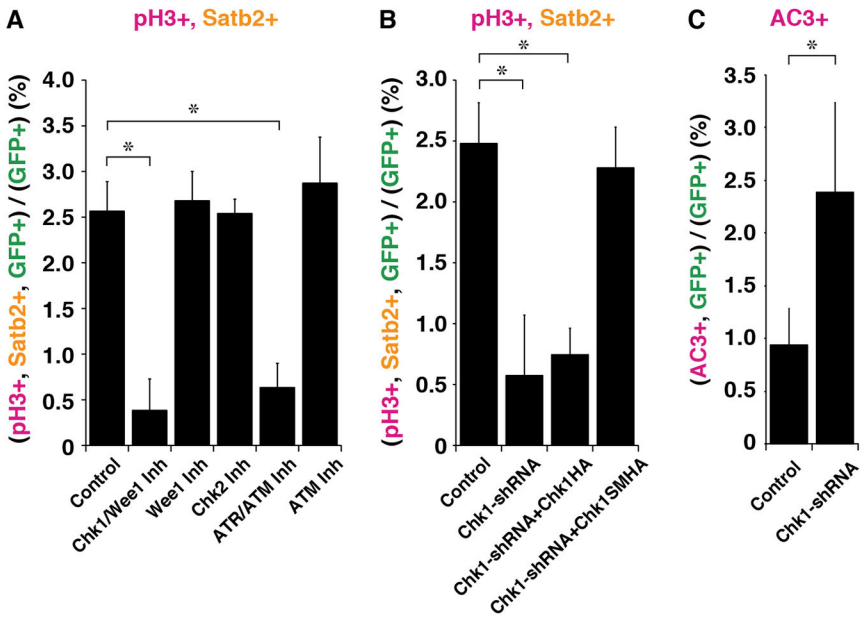


**Fig. 3. Essential role for Chk1 in CAG-Rb-TKO neuron survival and division.** (A-C) At 4 DIC (A,B) and 5 DIC (C), cortical explants were dissociated, plated on chamber slides, fixed and immunostained. (A-C) Cell scoring of pH3 and Satb2 (A,B), and of AC3 (C) immunopositive cells. Inh, inhibitor; SM, silent mutant. Data are mean±s.e.m. *$P$<0.05.

### Dnmt1 suppresses Chk1 pathway activation during neurogenesis

To determine the mechanism by which postmitotic neurons acquire protection from Chk1 pathway activation and subsequent cell division even after acute Rb family inactivation, we focused on the DNA methyltransferase Dnmt1, which blocks Chk1 pathway activation during the S phase (Unterberger et al., 2006) and is enriched in the cortical ventricular and subventricular zone (V/SVZ) (Visel et al., 2004). During neurogenesis, progenitor daughter cells undergo various epigenetic modifications, including DNA methylation (Yao and Jin, 2014). The Rb family directly and indirectly associates with various epigenetic modifiers and coordinates cell-cycle exit and neuronal differentiation by regulating epigenetic modifications (Burkhart and Sage, 2008). To compare the methylation status of the CAG- and MAP2-Rb-TKO cells, we performed 5-methylcytosine (5mC) immunostaining on cortical explants. The proportion of 5mC-positive cells was lower in the CAG-Rb-TKO than in the CAG-Rb-single explants, but the proportion was the same in the MAP2-Rb-TKO and MAP2-Rb-single explants (Fig. 5A-C). Overexpressing Dnmt1-shRNA in neural progenitors, which suppressed Dnmt1 expression (Fig. S7A), decreased the proportion of 5mC-positive MAP2-Rb-TKO cells (Fig. 5D) and increased that of pChk1-, and pChk2-positive MAP2-Rb-TKO cells (Fig. 5E, Fig. S7B). More than 75% of each of these cell populations was also EdU-positive (Fig. S7C), suggesting that Dnmt1 suppression induced Chk1/2 pathway activation during the S phase. Overexpressing Dnmt1-shRNA in MAP2-Rb-TKO cells decreased the proportion of AC3-positive cells (Fig. 5F) and increased that of pH3-positive and BrdU/EdU double-positive cells in a Chk1-dependent manner (Fig. 5G, Fig. S7D). To address whether Dnmt1 is dispensable after cell-cycle exit, we treated the MAP2-Rb-TKO cortical explants with 5-aza-2-deoxycytidine (5-Aza), a specific Dnmt1 inhibitor, from the beginning of the explant culture or for 10 h before fixation. The treatment for 10 h did not increase the proportion of pH3/Satb2 double-positive cells (Fig. S7E). These results suggest that Dnmt1 acts during neurogenesis to protect differentiating neurons from S-phase Chk1 pathway activation and cell division.

### Chk1 pathway activation promotes the survival and division of hypoxic neurons

Because, in some cases, the Rb family is important for G2/M phase progression (Burkhart and Sage, 2008), 1 nM CPT neuronal division might occur only in an Rb-TKO genetic background. To determine whether these activators also function in wild-type neurons under pathophysiological conditions, we used the hypoxic oxygen-glucose deprivation (OGD) model, which is widely used as an *in vitro* model for stroke. OGD induces Rb phosphorylation in cultured neurons, resulting in S-phase progression followed by cell death (Yu et al., 2012). Wild-type cortical neurons were labeled by *in vitro* electroporation with pMAP2-Cre and Cre-reporter plasmids (Fig. 6A). OGD treatment increased the number of AC3-positive and AC3/EdU double-positive neurons 36 h after stimulation (Fig. S8A-C), suggesting that OGD neurons died after S-phase progression in our culture system. To determine whether Chk1 pathway activators could prevent the dying OGD neurons from undergoing cell death and allow them to divide, similar to their effect on MAP2-Rb-TKO neurons, we treated OGD neurons with 1 nM CPT. CPT treatment reduced the proportion of AC3-positive cells (Fig. 6B,C) and increased that of pH3/Satb2 double-positive cells (Fig. 6D,E); both of these effects were suppressed by the Chk1/Wee1 inhibitor (Fig. 6B-E). We did not analyze AC3/Satb2 double-positive cells because most of the dying cells lost their Satb2 immunoreactivity.

To exclude the possibility that cell death prevention simply led to cell division, we treated OGD cells with a pan-caspase inhibitor, Z-VAD-FMK. This treatment reduced the proportion of AC3-positive cells, but had no effect on that of pH3-positive cells (Fig. S8D,E). Chk1 overexpression also had no effect on the proportion of pH3-positive cells (Fig. S8F). To determine whether 1 nM CPT would induce OGD neurons to divide after G2/M phase progression, we performed time-lapse imaging on dissociated OGD neurons (Fig. 6A). We found that the 1 nM CPT-treated OGD neurons underwent cell division, while maintaining their neurites (Fig. 6F, Movie 3). The daughter cells were both Satb2 positive (Fig. 6G), suggesting that neuronal division occurred without de-differentiation. These results suggested that the OGD neurons escaped cell death and divided after CPT treatment.

Finally, we examined whether 1 nM CPT promotes the division of OGD neurons *in vivo*. As hypoxia-ischemia treatment *in vivo*

Development (2017) 144, 3303-3314 doi:10.1242/dev.154013

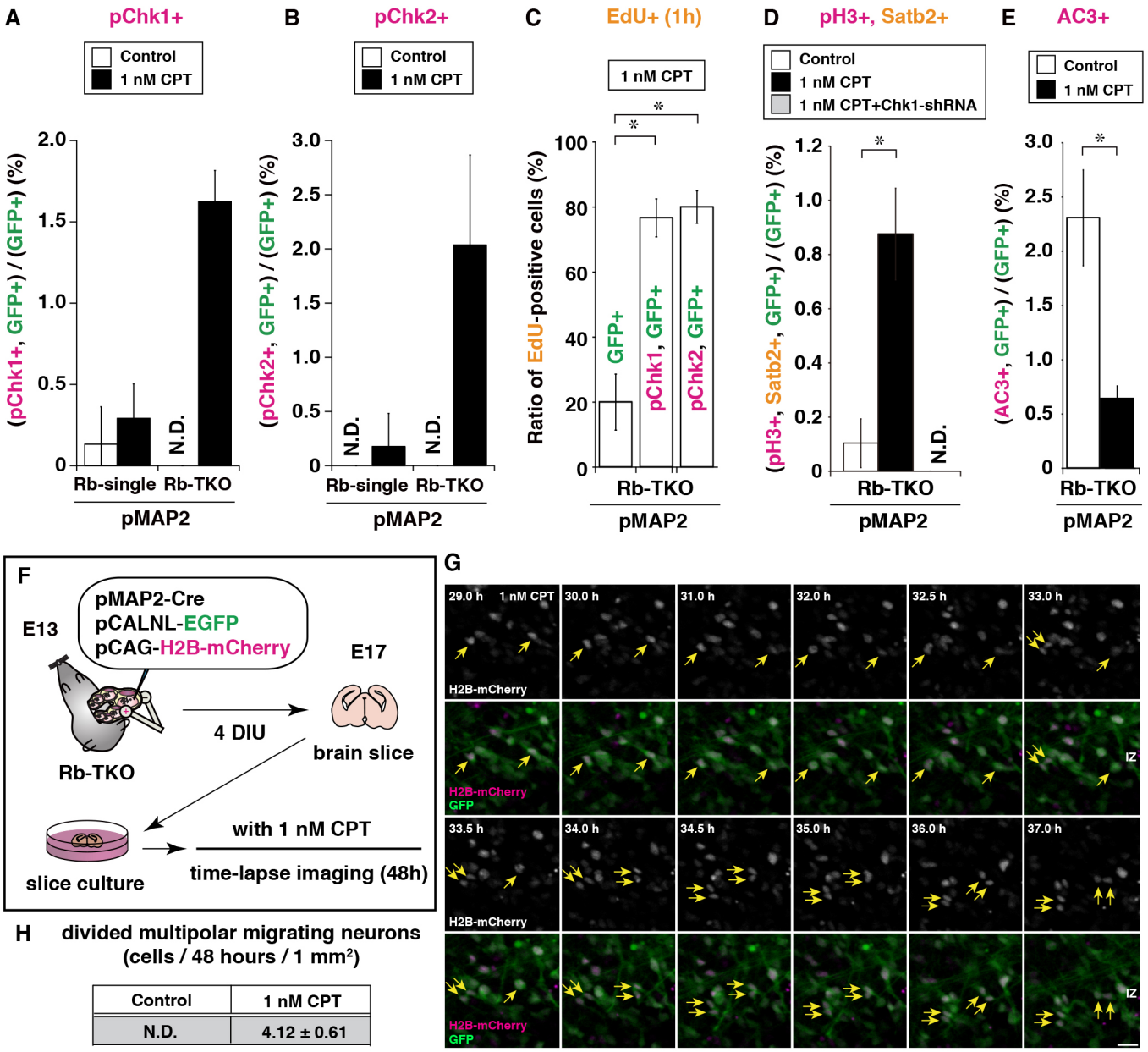


H divided multipolar migrating neurons (cells / 48 hours / 1 mm²)

| Control | 1 nM CPT |
|---|---|
| N.D. | 4.12 ± 0.61 |

**Fig. 4. Chk1 pathway activation promotes MAP2-Rb-TKO neuron survival and division.** (A-E) Cell scoring of immunopositive cells. (A-C) At 4 DIC after Cre-expressing plasmid electroporation, cortical explants were fixed, cryosectioned and immunostained. (D,E) At 4 (D) and 5 (E) DIC, cortical explants were dissociated, plated on chamber slides, fixed and immunostained. (F) Experimental design for time-lapse imaging of the brain slice. (G) Cell division observed in multipolar migrating neurons (arrows) in the IZ after stimulation with 1 nM CPT. (H) The number of divided multipolar migrating neurons in the presence or absence of 1 nM CPT. Scale bar: 25 µm. Data are mean±s.e.m. *$P$<0.05. IZ, intermediate zone.

causes neurons to re-enter the S phase and undergo cell death in the area surrounding the injured core (Katchanov et al., 2001), we performed distal middle cerebral artery occlusion (dMCAO) followed by hypoxia (Fig. 7A). After 1 nM CPT injection, pH3/Satb2 double-positive cells were detected in the hypoxia-ischemia mice (Fig. 7B-G). In contrast, without 1 nM CPT injection, we did not observe pH3/Satb2 double-positive cells (Fig. 7G). These results suggest that the OGD neurons *in vivo* were induced to divide by 1 nM CPT injection.

## DISCUSSION

As differentiation and proliferation remain tightly regulated in postmitotic neurons, even in pathological situations, neurons that progress through the S phase undergo cell death rather than division. Here, we have shown that cortical neurons became less susceptible to Chk1 pathway activation during neurogenesis in an Rb family- and Dnmt1-dependent manner, and thereby acquired mitotic resistance. Chk1 pathway activation also protected hypoxic cortical neurons in the S phase from undergoing cell death and induced their division. Based on these findings, we propose that Chk1 pathway activation during the S phase uncouples neuronal differentiation from mitotic resistance.

### The role of Chk1 in neuronal survival and division

Our findings, together with those of previous studies, show that acute Rb inactivation in differentiating neurons promotes their

Development (2017) 144, 3303-3314 doi:10.1242/dev.154013

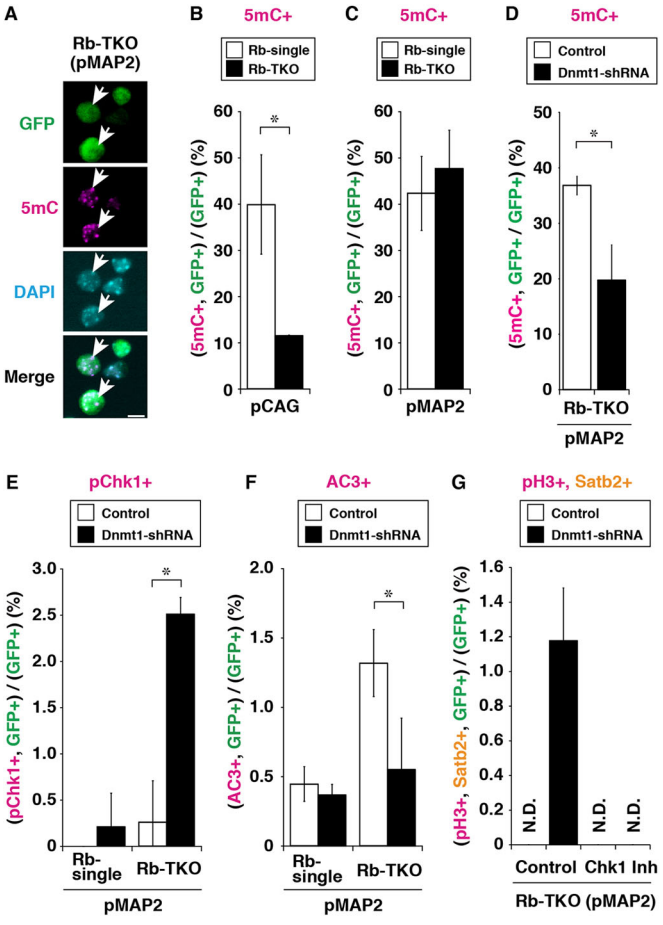


**Fig. 5. *Dnmt1* knockdown promotes Chk1-dependent MAP2-Rb-TKO neuron survival and division.** (A) GFP (green) and 5 mC (magenta) immunofluorescence images of MAP2-Rb-TKO cells. Nuclei were stained using DAPI (cyan). Arrows indicate immunopositive cells. (B-G) Cell scoring of immunopositive cells: cortical explants dissociated, plated on chamber slides, fixed and immunostained at 5 DIC (A-D,F,G); cortical explants were fixed, cryosectioned and immunostained at 4 DIC (E). Scale bar: 5 µm. Data are mean±s.e.m. *$P$<0.05.

entrance into the S phase, but results in cell death rather than cell division. Here, we have found that Chk1 pathway activation overrides mitotic resistance in neurons that have undergone acute Rb family inactivation (MAP2-Rb-TKO) and in those exposed to OGD. The Chk1 protein has multiple functions: besides its role in cell-cycle arrest, it is essential for the survival and proliferation of mouse ES cells (Liu et al., 2000; Takai et al., 2000) and MEFs (Naruyama et al., 2008; Shimada et al., 2008). Our finding that the Chk1 pathway was essential for the survival and division of CAG-Rb-TKO immature neurons was not surprising. However, our finding that postmitotic MAP2-Rb-TKO and OGD neurons could divide after Chk1 activation was unexpected, as cell-cycle exit is thought to be tightly linked with the loss of proliferative potency in postmitotic neurons.

Our study indicates that canonical Chk1 pathway is not important for MAP2-Rb-TKO cell division. There are several mechanisms by which Chk1-activated neurons divide after re-entering the cell cycle. One involves the regulation by Chk1 of genes required for cell division. Chk1 regulates the phosphorylation of histone H3 at threonine 11 (H3T11), which enhances cyclin b1 (*Ccnb1*) and *Cdk1* transcription by recruiting the GCN5 histone acetyltransferase (Shimada et al., 2008). An alternative, but not mutually exclusive, possibility involves the function of Chk1 in regulating the precise timing of cell division after S-phase progression, which prevents cell death (Canman, 2001; Ma et al., 2011). This possibility is supported by our analysis of DNA content and EdU/AC3 double staining, which revealed that MAP2-Rb-TKO and OGD neurons did not undergo S-phase arrest, but progressed through S phase before undergoing cell death. In addition, Chk1 positively regulates EGF signaling by inhibiting the function of the tumor suppressor Mig6 (Liu et al., 2012). Together, we propose that Chk1-mediated pathway regulation in S phase controls neuronal survival and division.

### Roles of the Rb family proteins and Dnmt1 in establishing mitotic resistance in cortical neurons during neurogenesis

Differentiating neurons become mitotically resistant immediately after exiting the cell cycle. Here, we have found that immature cortical neurons acquire mitotic resistance in an Rb family- and Dnmt1-dependent manner. The Rb family, which prevents S phase cell-cycle progression by suppressing E2F transcriptional activity, also regulates epigenetic modifications and is involved in stabilizing the genome to prevent tumor formation (Manning and Dyson, 2012; Talluri and Dick, 2012). We have recently found that Rb family inactivation in dividing progenitor cells prevents daughter cells from exiting the cell cycle, but allows them to differentiate and then proliferate (Oshikawa et al., 2013). In contrast, Rb family inactivation in postmitotic immature neurons causes their re-entry into the cell cycle and their subsequent death after S phase. These results indicate a crucial role for the Rb family during neurogenesis. Among the various epigenetic modifiers, we focused on Dnmt1 because Dnmt1 localizes to replication forks, and *Dnmt1* loss activates the Chk1 pathway during S phase (Unterberger et al., 2006). We show here that daughter neurons generated from Rb-TKO progenitor/*Dnmt1*-knockdown cells exhibit increased Chk1 pathway activation during S-phase progression, allowing them to escape cell death and divide. Although Dnmt1 activity is known to be regulated by binding to Rb (Pradhan and Kim, 2002; Robertson et al., 2000), these proteins were not colocalized in cortical progenitor cells in S phase (data not shown), suggesting that the direct interaction of Rb and Dnmt1 may not be important for the establishment of mitotic resistance. Although future studies are required for understanding how the Rb family regulates proper DNA methylation, our study suggested that the Rb family and Dnmt1 help establish mitotic resistance and mediate the cell-cycle exit of differentiating neurons.

### Effect of Rb family inactivation on the differentiation and survival of cortical neurons

Rb phosphorylation, which causes cell-cycle re-entry and subsequent cell death, plays an important role in the progression of neuronal disorders (Biswas et al., 2007; Nguyen et al., 2003; Silva et al., 2014; Yu et al., 2012). These findings are consistent with the seminal discoveries that Purkinje cells in the cerebellum and photoreceptor cells in the retina overexpressing SV40 large T-antigen undergo S-phase progression followed by cell death (al-Ubaidi et al., 1992; Feddersen et al., 1995, 1992). In contrast, Rb family inactivation causes unregulated neuronal proliferation in some cases. Mouse horizontal/amacrine cells and human cone photoreceptors can proliferate and form tumors when their respective neuronal progenitors have undergone Rb family inactivation or *RB1*-inactivating mutations, respectively (Ajioka et al., 2007; Chen et al., 2004; Xu et al., 2014). However, similarly inactivated neuronal progenitors generate rod photoreceptors, bipolar cells and ganglion cells that undergo cell death (Chen

Development (2017) 144, 3303-3314 doi:10.1242/dev.154013

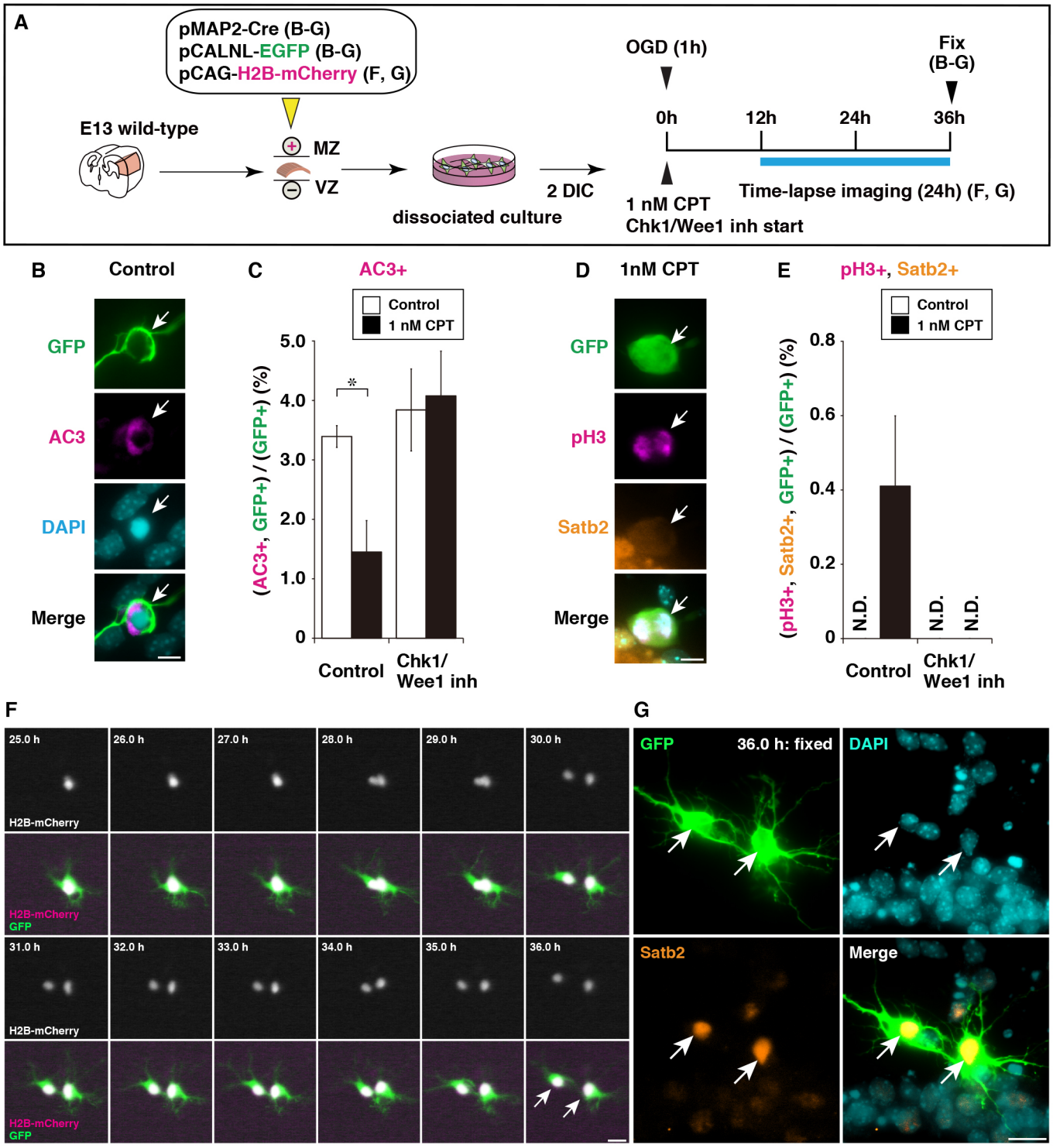


**Fig. 6. Chk1 pathway activation promotes OGD neuron survival and division.** (A) Experimental design. (B,D) Immunofluorescence staining of OGD neurons treated with (D) or without (B) 1 nM CPT for GFP (green), AC3 (B) and pH3 (D) (magenta), and Satb2 (D) (orange). Nuclei were stained using DAPI (cyan). Arrows indicate immunopositive cells. Scale bars: 5 µm. (C,E) Cell scoring of immunopositive cells. (F) Time-lapse imaging of dividing OGD neurons (arrows) after stimulation with 1 nM CPT. (G) GFP (green) and Satb2 (orange) immunofluorescence images of the OGD neurons, immediately after time-lapse imaging. Nuclei were stained using DAPI (cyan). Arrows in F,G indicate the same cells. VZ, ventricular zone; MZ, marginal zone; N.D., not detected. Scale bars: 10 µm. Data are mean±s.e.m. *$P$<0.05.

et al., 2004; MacPherson et al., 2004). These findings suggest a cell type-specific role for the Rb family in the retina (Ajioka and Dyer, 2008). Indeed, *Rb*-deficient rod photoreceptors fail to mature in a cell-autonomous manner (Johnson et al., 2006; Zhang et al., 2004), suggesting that in some cases neuronal death may be a secondary effect of abnormal development.

The experimental model used in this study has advantages for specifically addressing cell-death mechanisms that occur after

Development (2017) 144, 3303-3314 doi:10.1242/dev.154013

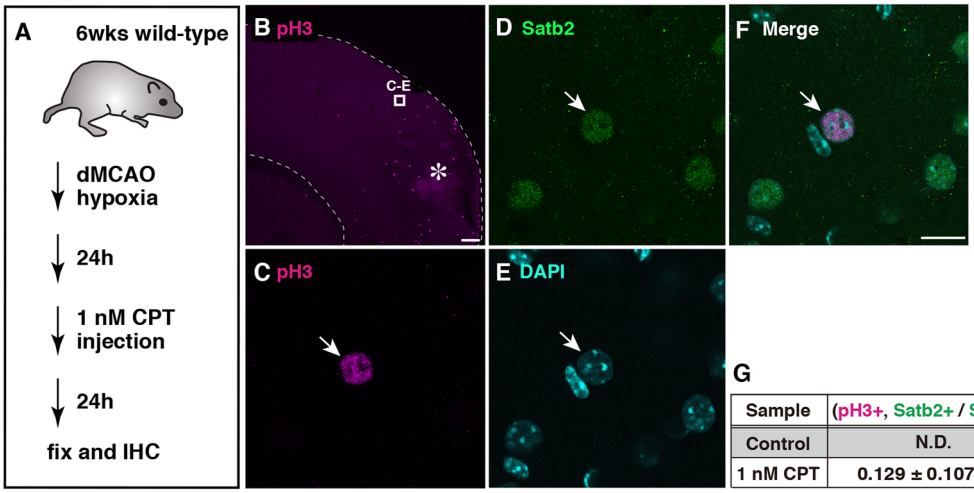


**Fig. 7. Chk1 pathway activation promotes neuron division in mouse stroke model.** (A) Experimental design for mouse stroke model. (B-E) Immunofluorescence staining of the ischemic cerebral cortex injected with 1 nM CPT for pH3 (B,C) and Satb2 (D) (green). Nuclei were stained using DAPI (cyan) (E) and these images were merged (F). Asterisks in B indicate the injured core. Arrows indicate immunopositive cells. Scale bars: 200 µm in B; 10 µm in F. (G) Cell scoring of immunopositive cells with and without 1 nM CPT injection. Data are mean±s.e.m. We analyzed five independent animals and performed cell scoring as described in the Materials and Methods. dMCAO, distal middle cerebral artery occlusion. i.p., intraperitoneal injection.

S-phase progression. First, our system, in which the entire family of Rb proteins was inactivated, overcomes the compensations and redundancies in the Rb family, and the acute inactivation of the Rb family leads to more rapid cell death than that of *Rb* inactivation, which induces neuronal death after 4 weeks (Andrusiak et al., 2012). In addition, most of the CAG-Rb-TKO and the MAP2-Rb-TKO cells are relatively homogeneous populations of cortical upper layer Satb2-positive neurons.

Although CAG-Rb-TKO immature neurons expand after several rounds of cell division *in vivo* (Oshikawa et al., 2013), we did not observe neuronal tumors in this model. Cortical neurons may be more protected from forming tumors than retinal neurons, as evidenced by the large number of individuals with retinoblastoma. As dividing cortical neurons appear to be less tumorigenic, it will be interesting to investigate the potential therapeutic effects of ectopic Chk1 pathway activation for stroke and neurodegenerative disorders.

## MATERIALS AND METHODS

### Mice

The $Rb^{Lox/Lox}$; $p107^{-/-}$; $p130^{Lox/Lox}$ mice were obtained from Dr Michael Dyer (St. Jude Children's Research Hospital). The $Rb^{Lox/Lox}$ mice and *p107*-knockout mice were originally produced by Dr Tyler Jacks (Massachusetts Institute of Technology). The $p130^{Lox/Lox}$ and *Z/EG* mice were originally produced by Dr Julien Sage (Stanford University) and Dr Corrinne Lobe (Miami Mice Research Corp.), respectively. Wild-type ICR and C57BL/6J mice were purchased from SLC (Shizuoka, Japan). All experimental procedures involving animals were approved by the Animal Experiment Committee of Tokyo Medical and Dental University and the Aichi Human Service Center.

### Plasmid construction

The primers used in this study are listed in Table S1. To generate an HA-tagged Chk1 expression construct, we generated a pCAG-CASSETTE (CST)-HA plasmid with a *Not*I site for inserting the HA-tagged sequence. The pCAGGS plasmid (Niwa et al., 1991) was digested using *Eco*RI and inserted as follows to generate pCAG-CST-HA: 5′-AATTCGCTAGCTC-TAGAATGGCGGCCGCATACCCATACGATGTTCCAGATTACGCTT-AATCTAG-3′. To generate pCAG-Chk1-HA, pCAG-Dnmt1-HA and pCAG-Cdc25A, the mouse Chk1, Dnmt1, Cdc25A cDNAs were amplified using the Chk1-Fw and Chk1-Rv primers, Dnmt1-Fw and Dnmt1-Rv primers, and Cdc25A-Fw and Cdc25A-Rv primers, respectively, from E16 mouse cerebral cortex cDNA, and the resulting PCR products were inserted into the *Not*I site of pCAG-CST-HA. To generate pCAG-Chk1SM-HA, in which the Chk1 cDNA has silent mutations in the L25, N28 and R29 codons, Chk1 (L25L) cDNA was amplified from pCAG-Chk1-HA using the PrimeSTAR Mutagenesis Basal Kit (TaKaRa; Shiga, Japan) with the Chk1-SM-Fw2.2 and Chk1-SM-Rv2.2 primers. Next, Chk1 (L25L, N28N and R29R) cDNA was amplified from pCAG-Chk1(L25L)-HA using the PrimeSTAR Mutagenesis Basal Kit with the Chk1-SM-Fw3 and Chk1-SM-Rv3 primers. To generate a pCALNL-HA-Chk1(L449R) plasmid, in the first step, HA-tagged Chk1(L449R) cDNA was amplified from pCAG-Chk1-HA using the QuikChange Site-Directed Mutagenesis Kit (Stratagene) with the Chk1-L449R-Fw and Chk1-L449R-Rv primers. In the second step, to generate pCAG-HA-Chk1(L449R) cDNA, Chk1-L449R cDNA and pCAG-HA cDNA were amplified using the ha-Chk1-Fw and ha-Chk1-Rv and HAvector-*Mfe*I-Fw and HAvector-*Sac*I-Rv primers, respectively, and then digested using *Mfe*I and *Sac*I; the pCAG-HA-Chk1-L449R plasmid was then obtained by ligating these fragments. In the third step, to generate pCALNL-HA-Chk1(L449R), the *Eco*RI and PspOM I-ligated HA-Chk1-L449R cDNA was amplified using the CAG-seq-Fw and ha-Chk1-Rv2 primers. To replace the GFP cDNA in the pCALNL-GFP plasmid with HA-Chk1-L449R cDNA, pCALNL-GFP was digested using *Eco*RI and *Not*I, after which the *Eco*RI- and PspOM-ligated HA-Chk1-L449R cDNA was inserted into the pCALNL vector. To generate pSilencer-Chk1, annealed Chk1-si-Fw1 and Chk1-si-Rv1 oligo DNAs (Gasser et al., 2005) (Table S1) were inserted into the *Apa*I and *Eco*RI sites of pSilencer 1.0. To generate pSilencer-Dnmt1, annealed Dnmt1-si-Fw3 and Dnmt1-si-Rv3, and Dnmt1-si-Fw9 and Dnmt1-si-Rv9 oligo DNAs (Table S1) were inserted into the *Apa*I and *Eco*RI sites of pSilencer 1.0, respectively. A mixture of the two different Dnmt1 shRNA-expressing plasmids was used in the experiments. The Dnmt1 target sequences were obtained from The RNAi Consortium (www.broadinstitute.org).

### *Ex vivo* electroporation

The dissected cerebral cortex from E13 mice was transferred to a Petri dish electrode chamber (CUY520P5, Nepagene) filled with plasmid solution and was transfected using 25 V square-pulse electroporation (NEPA21, Nepagene) (Oshikawa et al., 2013). The *ex vivo* transfected cerebral cortex was transferred to a polycarbonate membrane (Whatman) in explant medium [Dulbecco's Modified Eagle Medium: Nutrient Mixture F-12 Medium (Sigma) supplemented with 10% fetal bovine serum (Thermo Fisher Scientific), 10 mM HEPES (Thermo Fisher Scientific), penicillin/

Development (2017) 144, 3303-3314 doi:10.1242/dev.154013

streptomycin/glutamine (Thermo Fisher Scientific), and insulin (Sigma)], and was cultured. For EdU labeling, 10 µg/ml EdU was added for 1, 16 or 24 h before fixation. For shRNA experiments, we used a Cre reporter-GFP plasmid (pCALNL-EGFP), instead of a *Z/EG* transgene, to detect shRNA-transfected Rb-TKO cells. The transfected cerebral cortex was cultured for 4 and 5 days in the presence or absence of 2 µM Wee1/Chk1 inhibitor (681637, Merck), 10 µM Wee1 inhibitor (681641, Merck), 10 µM Chk2 inhibitor (220486, Merck), 10 µM ATR/ATM inhibitor (118501, Merck) or 10 µM ATM inhibitor (118500, Merck) for 16 h before fixation, in the presence of 1 nM CPT (Sigma) after 3 DIC.

### *In utero* electroporation

pCAG-Cre and pMAP2-Cre were injected into the lateral ventricle of E13 mouse embryos. The cells attached to the ventricular surface were transfected using 35 V square-pulse electroporation (NEPA21; Nepagene), as described previously (Tabata and Nakajima, 2001). For double BrdU and EdU labeling, 50 µg/g bodyweight of BrdU (Sigma) was injected intraperitoneally at E17, followed by the same amount of EdU (Thermo Fisher Scientific) 24 h later. At E17 or E18 (1 h after BrdU or EdU injection), the transfected mice were fixed by perfusion with 4% paraformaldehyde, and the brains were cryosectioned. For AC3 immunostaining, EdU was injected four times every 3 h at E17, and the transfected mice were fixed 24 h after the final EdU injection.

### Immunohistochemistry

The following antibodies were used for immunohistochemistry: chicken anti-GFP (1:1000, ab13970, Abcam), rabbit anti-TBR2 (1:500, ab23345, Abcam), rabbit anti-pChk1 (Ser317) (1:800, 12302, Cell Signaling), rabbit anti-pChk2 (1:100, 2661, Cell Signaling), mouse anti-SATB2 (1:100, ab51502, Abcam), rat anti-phospho S28 histone H3 (1:300, ab10543, Abcam) and mouse anti-BrdU (1:1000, 555627, BD Bioscience). For BrdU staining, the cryosections were pre-treated with 2 N HCl for 10 min. For immunohistochemical analysis, cryosections were post-fixed in 4% paraformaldehyde for 3 h at 4°C, pre-incubated with 2% normal goat serum for 1 h at room temperature, and incubated with one of the above antibodies overnight at 4°C. The primary antibodies were visualized using Alexa Fluor 488-labeled goat anti-chicken IgG (Thermo Fisher Scientific), Alexa Fluor 546-labeled goat anti-mouse, anti-rabbit and anti-rat IgGs (Thermo Fisher Scientific), and Alexa Fluor 647-labeled goat anti-mouse IgG (Thermo Fisher Scientific). EdU-incorporated cells were visualized using Alexa Fluor 647 after the primary antibody reaction. The nuclei were counterstained with 2 µg/ml DAPI (Sigma). Fluorescence images were obtained using a confocal microscope (Fv10i; Olympus). To count the EdU- or Satb2-positive cells among the double-positive cells expressing both GFP and pChk1, or pChk2 alone, we randomly selected 20 double-positive cells in three different regions.

### Immunocytostaining

For cell dissociation, explant tissues were treated with 100 µg/ml trypsin (Sigma) in $Ca^{2+}$- and $Mg^{2+}$-free phosphate-buffered saline (PBS) for 5 min at 37°C. After gentle tapping, the cells were incubated for an additional 5 min at 37°C and were then dissociated by tapping. Next, the cells were incubated with 100 µg/ml trypsin inhibitor (Sigma) and 20 µg/ml DNase (Sigma) in PBS with $Ca^{2+}$ and $Mg^{2+}$ for 5 min at 37°C. After adding five volumes of explant medium, the cells were plated on poly-L-lysine (Sigma)-coated glass slides (Millicell EZ, Merck) and incubated for 1 h at 37°C. The cells were attached to the slides by centrifugation at 500 ***g*** at room temperature and then fixed with 4% PFA for 1 h at 4°C. The fixed cells were pre-incubated with 2% normal goat or donkey serum for 1 h at room temperature, and incubated with chicken anti-GFP (1:1000), rabbit anti-SATB2 (1:100, ab92446, Abcam), mouse anti-nestin (1;1000, 556309, BD Pharmingen), mouse anti-BrdU, rat anti-phospho S28 histone H3 (1:300), rabbit anti-AC3 (1:200, AB3623, Merck), goat anti-Olig2 (1:1000, AF2418, R&D Systems) or mouse anti-5mC (ab10805, Abcam). For BrdU and 5mC staining, the cryosections were pre-treated with 2 N HCl for 10 and 30 min, respectively. The primary antibodies were visualized using Alexa Fluor 488-labeled goat anti-chicken IgG, Alexa Fluor 546-labeled goat anti-mouse, anti-rabbit and anti-rat IgGs, and Alexa Fluor 647-labeled goat anti-mouse and donkey anti-goat IgGs. EdU-incorporated cells were visualized using Alexa Fluor 647 after the primary antibody reaction. The nuclei were counterstained with 2 µg/ml DAPI (Sigma). Fluorescence images were captured using a fluorescence microscope (IX73, Olympus) and a CCD camera (C10600-10B, Hamamatsu Photonics).

### Cell counting using 2D and 3D stereology

The immunopositive cells were counted by unbiased 2D and 3D stereology (Stereo Investigator, MBF Bioscience) for dissociated cells and sectioned tissues, respectively. For 2D stereology, a counting frame of 200×200 µm was used in 400×400 µm matrices for pH3 and AC3 staining, and in 800×800 µm matrices for all other staining. For 3D stereology, a counting frame of 100×100×10 µm was used in 300×300 µm matrices in each 400 µm section. Fluorescence images were captured using a fluorescence microscope (IX73, Olympus) and a CCD camera (C10600-10B, Hamamatsu Photonics). Data are presented as the mean±s.e.m. with $n$=3 for explant and $n$=5 for dMCAO biological replicates. Comparisons of data were analyzed using Student's $t$-test.

### DNA content measurement

DNA content was measured using microphotometry with the MetaMorph software Cell-Cycle Application Module (Molecular Devices) (Ikenishi et al., 2012). Approximately 500 GFP-positive nuclei were analyzed and plotted, and the statistical data were obtained from three independent experiments.

### Western blotting

The transfected 293 T cells were lysed in lysis buffer [20 mM Tris (pH 7.4), 150 mM NaCl, 1 mM ethylene-diamine-tetra-acetic acid (EDTA), 1% NP-40 and protease inhibitor (cOmplete EDTA-free, Roche)] and the samples were centrifuged at 15,000 ***g*** for 5 min. The supernatants were mixed with SDS loading buffer and subjected to SDS-PAGE on 7.5% and 12% polyacrylamide gels. The proteins were then electroblotted onto polyvinylidene fluoride membranes using an iBlot Gel Transfer Device (Thermo Fisher Scientific). The membranes were incubated with mouse anti-HA (1:5000, ab9110) and mouse anti-β actin (1:10,000, ab6276, Abcam) for 16 h at 4°C after blocking with 5% skimmed milk for 1 h at room temperature, and then with peroxidase-labeled goat anti-mouse and anti-rabbit IgG (1:5000, Dako) for 2 h. The bands were detected using SuperSignal West Femto Maximum Sensitivity Substrate (Thermo Fisher Scientific) and were visualized using a Sayaca-Imager (DRC).

### Real-time PCR analysis

For the sorting of Rb-TKO cells, the GFP-positive cells were dissociated from 4 DIC explants, labeled with 100 ng/ml of DAPI to remove dead cells and then sorted using a FACS Vantage SE (BD Bioscience). First-strand cDNA was synthesized from 1 µg of total RNA from GFP-positive cells, retinoblastoma cell lines and retinal tissues with 100 pmol of T7-(dT)24 primer and 200 units of Superscript III (Thermo Fisher Scientific) at 42°C for 1 h. The real-time RT-PCR was performed using SsoFast Probes Supermix (Bio-Rad) and the CFX96 system (Bio-Rad). The primer sequences are shown in Table S2. The gene expression levels were normalized to the *Gapdh* and *Gpi1* expression levels.

### Time-lapse imaging of brain slice cultures

pCAG-Cre and pMAP2-Cre were injected into the lateral ventricle of E13 mouse embryos. The cells attached to the ventricular surface were transfected using 35 V square-pulse electroporation (NEPA21; Nepagene), as described previously (Tabata and Nakajima, 2001). Time-lapse imaging of brain slice cultures was performed as previously described (Tabata and Nakajima, 2003).

### Real-time PCR analysis

For the sorting of Rb-TKO cells, the GFP-positive cells were dissociated from 4 DIC explants, labeled with 100 ng/ml of DAPI to remove dead cells, and then sorted using a FACS Vantage SE (BD Bioscience). First-strand cDNA was synthesized from 1 µg of total RNA from GFP-positive cells,

Development (2017) 144, 3303-3314 doi:10.1242/dev.154013

retinoblastoma cell lines and retinal tissues with 100 pmol of T7-(dT)24 primer and 200 units of Superscript III (Thermo Fisher Scientific) at 42°C for 1 h. The real-time RT-PCR was performed using SsoFast Probes Supermix (Bio-Rad) and the CFX96 system (Bio-Rad). The primer sequences are shown in Table S2. The gene expression levels were normalized to the *Gapdh* and *Gpi1* expression levels.

### OGD stimulation

We modified the OGD stimulation method reported previously (Yu et al., 2012). E13 wild-type cerebral cortices were dissociated with 1 mg/ml trypsin (Sigma). The dissociated cortical cells ($5\times10^5$ cells) were plated on Engelbreth-Holm-Swarm sarcoma (EHS) laminin (Sigma)-coated 13 mm coverglasses (Matsunami) and cultured in neuron medium [1:1 mixture of Dulbecco's modified Eagle medium/Nutrient Mixture F-12 medium (DMEM/F-12) (Sigma) and Neurobasal medium (Thermo Fisher Scientific) supplemented with N2 (Thermo Fisher Scientific), B27 (Thermo Fisher Scientific), GlutaMAX (Thermo Fisher Scientific), minimum essential media (MEM) Non-Essential Amino Acids (NEAA) Solution (Thermo Fisher Scientific), 2.5 µg/ml insulin (Sigma), 1% 2-mercaptoethanol (Sigma)] in the presence of 10 µM 5-fluoro-2′-deoxyuridine and 10 µM uridine. After a 2-day culture, the cells were cultured in an incubator chamber (5% $CO_2$ and 1% $O_2$ at 37°C) (INUBTF-WSKM, Tokai Hit and TK-MIGM01-O2T, Tokken) with Earle's Balanced Salt Solution (EBSS) without glucose in the presence of 10 µM MK-801 for 1 h. Immediately after OGD stimulation, the medium was replaced with neuron medium containing 10 µM MK-801 and the cells were cultured in a 5% $CO_2$ incubator. We performed immunostaining for Olig2 to exclude the possibility of counting glial progenitor cells.

### Time-lapse imaging of dissociated neurons

Dissociated cortical cells were cultured on Engelbreth-Holm-Swarm sarcoma (EHS) laminin (Sigma)-coated 35 mm glass-bottomed dishes (AGC Techno Glass) for 2 days in a 5% $CO_2$ incubator. Cortical cells were cultured in neuron medium in the presence of 10 µM 5-fluoro-2′-deoxyuridine (Sigma) and 10 µM uridine (Sigma). After OGD stimulation for 1 h, the cells were cultured in neuron medium with 10 µM MK-801 (Sigma) and 1 nM CPT (Sigma) for 12 h in a 5% $CO_2$ incubator. The dishes were then placed in an incubation chamber (5% $CO_2$ at 37°C) fitted onto a fluorescence microscope (IX73, Olympus), and five optimal *z* sections were obtained automatically every 30 min using a CCD camera (C10600-10B, Hamamatsu Photonics) and cellSens software (Olympus) for 24 h. Immediately after time-lapse imaging, the cells were fixed and immunostained.

### Mouse hypoxic stroke model

The mouse dMCAO and hypoxic model was produced as previously described (Oshikawa et al., 2017). Briefly, 6-week-old of C57BL/6J mice were deeply anesthetized by spontaneous inhalation of isoflurane, and temporalis muscle was removed. The right middle cerebral artery (MCA) was exposed by using an Ideal Micro-Drill (CellPoint Scientific) and the vessel was cauterized using a small vessel cauterizer (Gemini Cautery Kit, CellPoint Scientific). After recovery, they were placed in a hypoxic chamber containing 8% $O_2$ and 92% $N_2$ using an $O_2$ controller (ProOx 110, Bio Spherix) for 1 h. After 24 h, these mice were deeply anesthetized by spontaneous inhalation of isoflurane. Finally, 1 µl of 1 nM CPT or control PBS was injected near the cauterized vessel using Hamilton Syringe (Hamilton).

### Statistics

Comparisons of data were analyzed using one-way ANOVA, followed by Student–Newman–Keuls test. All data are expressed as the mean±s.e.m.

#### Acknowledgements

We thank Drs Sawamoto and Kaneko for advice on the mouse stroke model. We also thank Drs Michael Dyer, Tyler Jacks, Julien Sage and Corrinne Lobe for genetically engineered mice, and Dr Vijayasaradhi Setaluri for the human MAP2 promoter DNA.

#### Competing interests

The authors declare no competing or financial interests.

#### Author contributions

Conceptualization: I.A.; Methodology: I.A., M.O., K.-i.N., H.T.; Formal analysis: I.A., M.O.; Investigation: I.A., M.O., K.O., K.-i.N., H.T.; Data curation: I.A., M.O., K.O.; Writing - original draft: I.A.; Writing - review & editing: I.A., M.O., H.T.; Supervision: I.A.; Project administration: I.A.; Funding acquisition: I.A.

#### Funding

This work was supported by the PRESTO program of the Japan Science and Technology Agency (JPMJPR14K1), a Grant-in-Aid for Scientific Research from the Ministry of Education, Culture, Sports, Science and Technology (MEXT) (JP15H03019), by the Canon Foundation and by the Terumo Foundation for Life Sciences and Arts.

#### Supplementary information

Supplementary information available online at
http://dev.biologists.org/lookup/doi/10.1242/dev.154013.supplemental

#### References

**Ajioka, I.** (2014). Coordination of proliferation and neuronal differentiation by the retinoblastoma protein family. *Dev. Growth Differ.* **56**, 324-334.

**Ajioka, I. and Dyer, M. A.** (2008). A new model of tumor susceptibility following tumor suppressor gene inactivation. *Cell Cycle* **7**, 735-740.

**Ajioka, I., Martins, R. A. P., Bayazitov, I. T., Donovan, S., Johnson, D. A., Frase, S., Cicero, S. A., Boyd, K., Zakharenko, S. S. and Dyer, M. A.** (2007). Differentiated horizontal interneurons clonally expand to form metastatic retinoblastoma in mice. *Cell* **131**, 378-390.

**al-Ubaidi, M. R., Hollyfield, J. G., Overbeek, P. A. and Baehr, W.** (1992). Photoreceptor degeneration induced by the expression of simian virus 40 large tumor antigen in the retina of transgenic mice. *Proc. Natl. Acad. Sci. USA* **89**, 1194-1198.

**Andrusiak, M. G., Vandenbosch, R., Park, D. S. and Slack, R. S.** (2012). The retinoblastoma protein is essential for survival of postmitotic neurons. *J. Neurosci.* **32**, 14809-14814.

**Angevine, J. B., Jr. and Sidman, R. L.** (1961). Autoradiographic study of cell migration during histogenesis of cerebral cortex in the mouse. *Nature* **192**, 766-768.

**Bartek, J. and Lukas, J.** (2003). Chk1 and Chk2 kinases in checkpoint control and cancer. *Cancer Cell* **3**, 421-429.

**Biswas, S. C., Shi, Y., Vonsattel, J.-P. G., Leung, C. L., Troy, C. M. and Greene, L. A.** (2007). Bim is elevated in Alzheimer's disease neurons and is required for beta-amyloid-induced neuronal apoptosis. *J. Neurosci.* **27**, 893-900.

**Blomberg, I. and Hoffmann, I.** (1999). Ectopic expression of Cdc25A accelerates the G(1)/S transition and leads to premature activation of cyclin E- and cyclin A-dependent kinases. *Mol. Cell. Biol.* **19**, 6183-6194.

**Burkhart, D. L. and Sage, J.** (2008). Cellular mechanisms of tumour suppression by the retinoblastoma gene. *Nat. Rev. Cancer* **8**, 671-682.

**Canman, C. E.** (2001). Replication checkpoint: preventing mitotic catastrophe. *Curr. Biol.* **11**, R121-R124.

**Chen, D., Livne-bar, I., Vanderluit, J. L., Slack, R. S., Agochiya, M. and Bremner, R.** (2004). Cell-specific effects of RB or RB/p107 loss on retinal development implicate an intrinsically death-resistant cell-of-origin in retinoblastoma. *Cancer Cell* **5**, 539-551.

**Cliby, W. A., Lewis, K. A., Lilly, K. K. and Kaufmann, S. H.** (2002). S phase and G2 arrests induced by topoisomerase I poisons are dependent on ATR kinase function. *J. Biol. Chem.* **277**, 1599-1606.

**Cole, K. A., Huggins, J., Laquaglia, M., Hulderman, C. E., Russell, M. R., Bosse, K., Diskin, S. J., Attiyeh, E. F., Sennett, R., Norris, G. et al.** (2011). RNAi screen of the protein kinome identifies checkpoint kinase 1 (CHK1) as a therapeutic target in neuroblastoma. *Proc. Natl. Acad. Sci. USA* **108**, 3336-3341.

**Dehay, C. and Kennedy, H.** (2007). Cell-cycle control and cortical development. *Nat. Rev. Neurosci.* **8**, 438-450.

**Dyer, M. A. and Cepko, C. L.** (2001). Regulating proliferation during retinal development. *Nat. Rev. Neurosci.* **2**, 333-342.

**Edlund, T. and Jessell, T. M.** (1999). Progression from extrinsic to intrinsic signaling in cell fate specification: a view from the nervous system. *Cell* **96**, 211-224.

**El-Khodor, B. F., Oo, T. F., Kholodilov, N. and Burke, R. E.** (2003). Ectopic expression of cell cycle markers in models of induced programmed cell death in dopamine neurons of the rat substantia nigra pars compacta. *Exp. Neurol.* **179**, 17-27.

**Feddersen, R. M., Ehlenfeldt, R., Yunis, W. S., Clark, H. B. and Orr, H. T.** (1992). Disrupted cerebellar cortical development and progressive degeneration of Purkinje cells in SV40 T antigen transgenic mice. *Neuron* **9**, 955-966.

**Feddersen, R. M., Clark, H. B., Yunis, W. S. and Orr, H. T.** (1995). In vivo viability of postmitotic Purkinje neurons requires pRb family member function. *Mol. Cell. Neurosci.* **6**, 153-167.

**Ferguson, K. L., Vanderluit, J. L., Hebert, J. M., McIntosh, W. C., Tibbo, E., MacLaurin, J. G., Park, D. S., Wallace, V. A., Vooijs, M., McConnell, S. K. et al.** (2002). Telencephalon-specific Rb knockouts reveal enhanced neurogenesis, survival and abnormal cortical development. *EMBO J.* **21**, 3337-3346.

**Florio, M. and Huttner, W. B.** (2014). Neural progenitors, neurogenesis and the evolution of the neocortex. *Development* **141**, 2182-2194.

**Gasser, S., Orsulic, S., Brown, E. J. and Raulet, D. H.** (2005). The DNA damage pathway regulates innate immune system ligands of the NKG2D receptor. *Nature* **436**, 1186-1190.

**Guillemot, F., Molnár, Z., Tarabykin, V. and Stoykova, A.** (2006). Molecular mechanisms of cortical differentiation. *Eur. J. Neurosci.* **23**, 857-868.

**Heintz, N.** (1993). Cell death and the cell cycle: a relationship between transformation and neurodegeneration? *Trends Biochem. Sci.* **18**, 157-159.

**Herrup, K. and Yang, Y.** (2007). Cell cycle regulation in the postmitotic neuron: oxymoron or new biology? *Nat. Rev. Neurosci.* **8**, 368-378.

**Hoglinger, G. U., Breunig, J. J., Depboylu, C., Rouaux, C., Michel, P. P., Alvarez-Fischer, D., Boutillier, A.-L., Degregori, J., Oertel, W. H., Rakic, P. et al.** (2007). The pRb/E2F cell-cycle pathway mediates cell death in Parkinson's disease. *Proc. Natl. Acad. Sci. USA* **104**, 3585-3590.

**Ikenishi, A., Okayama, H., Iwamoto, N., Yoshitome, S., Tane, S., Nakamura, K., Obayashi, T., Hayashi, T. and Takeuchi, T.** (2012). Cell cycle regulation in mouse heart during embryonic and postnatal stages. *Dev. Growth Differ.* **54**, 731-738.

**Johnson, D. A., Donovan, S. L. and Dyer, M. A.** (2006). Mosaic deletion of Rb arrests rod differentiation and stimulates ectopic synaptogenesis in the mouse retina. *J. Comp. Neurol.* **498**, 112-128.

**Katchanov, J., Harms, C., Gertz, K., Hauck, L., Waeber, C., Hirt, L., Priller, J., von Harsdorf, R., Bruck, W., Hortnagl, H. et al.** (2001). Mild cerebral ischemia induces loss of cyclin-dependent kinase inhibitors and activation of cell cycle machinery before delayed neuronal cell death. *J. Neurosci.* **21**, 5045-5053.

**Kriegstein, A. and Alvarez-Buylla, A.** (2009). The glial nature of embryonic and adult neural stem cells. *Annu. Rev. Neurosci.* **32**, 149-184.

**Kuan, C.-Y., Schloemer, A. J., Lu, A., Burns, K. A., Weng, W. L., Williams, M. T., Strauss, K. I., Vorhees, C. V., Flavell, R. A., Davis, R. J. et al.** (2004). Hypoxia-ischemia induces DNA synthesis without cell proliferation in dying neurons in adult rodent brain. *J. Neurosci.* **24**, 10763-10772.

**Lee, E. Y., Hu, N., Yuan, S. S., Cox, L. A., Bradley, A., Lee, W. H. and Herrup, K.** (1994). Dual roles of the retinoblastoma protein in cell cycle regulation and neuron differentiation. *Genes Dev.* **8**, 2008-2021.

**Liu, Q., Guntuku, S., Cui, X. S., Matsuoka, S., Cortez, D., Tamai, K., Luo, G., Carattini-Rivera, S., DeMayo, F., Bradley, A. et al.** (2000). Chk1 is an essential kinase that is regulated by Atr and required for the G(2)/M DNA damage checkpoint. *Genes Dev.* **14**, 1448-1459.

**Liu, N., Matsumoto, M., Kitagawa, K., Kotake, Y., Suzuki, S., Shirasawa, S., Nakayama, K. I., Nakanishi, M., Niida, H. and Kitagawa, M.** (2012). Chk1 phosphorylates the tumour suppressor Mig-6, regulating the activation of EGF signalling. *EMBO J.* **31**, 2365-2377.

**Ma, C. X., Janetka, J. W. and Piwnica-Worms, H.** (2011). Death by releasing the breaks: CHK1 inhibitors as cancer therapeutics. *Trends Mol. Med.* **17**, 88-96.

**MacPherson, D., Sage, J., Crowley, D., Trumpp, A., Bronson, R. T. and Jacks, T.** (2003). Conditional mutation of Rb causes cell cycle defects without apoptosis in the central nervous system. *Mol. Cell. Biol.* **23**, 1044-1053.

**MacPherson, D., Sage, J., Kim, T., Ho, D., McLaughlin, M. E. and Jacks, T.** (2004). Cell type-specific effects of Rb deletion in the murine retina. *Genes Dev.* **18**, 1681-1694.

**Manning, A. L. and Dyson, N. J.** (2012). RB: mitotic implications of a tumour suppressor. *Nat. Rev. Cancer* **12**, 220-226.

**Naruyama, H., Shimada, M., Niida, H., Zineldeen, D. H., Hashimoto, Y., Kohri, K. and Nakanishi, M.** (2008). Essential role of Chk1 in S phase progression through regulation of RNR2 expression. *Biochem. Biophys. Res. Commun.* **374**, 79-83.

**Nguyen, M. D., Boudreau, M., Kriz, J., Couillard-Despres, S., Kaplan, D. R. and Julien, J. P.** (2003). Cell cycle regulators in the neuronal death pathway of amyotrophic lateral sclerosis caused by mutant superoxide dismutase 1. *J. Neurosci.* **23**, 2131-2140.

**Niwa, H., Yamamura, K. and Miyazaki, J.** (1991). Efficient selection for high-expression transfectants with a novel eukaryotic vector. *Gene* **108**, 193-199.

**Oshikawa, M., Okada, K., Nakajima, K. and Ajioka, I.** (2013). Cortical excitatory neurons become protected from cell division during neurogenesis in an Rb family-dependent manner. *Development* **140**, 2310-2320.

**Oshikawa, M., Okada, K., Kaneko, N., Sawamoto, K. and Ajioka, I.** (2017). Affinity-immobilization of VEGF on laminin porous sponge enhances angiogenesis in the ischemic brain. *Adv. Healthc. Mater.* **6**, 201700183.

**Osuga, H., Osuga, S., Wang, F., Fetni, R., Hogan, M. J., Slack, R. S., Hakim, A. M., Ikeda, J.-E. and Park, D. S.** (2000). Cyclin-dependent kinases as a therapeutic target for stroke. *Proc. Natl. Acad. Sci. USA* **97**, 10254-10259.

**Pradhan, S. and Kim, G. D.** (2002). The retinoblastoma gene product interacts with maintenance human DNA (cytosine-5) methyltransferase and modulates its activity. *EMBO J.* **21**, 779-788.

**Robertson, K. D., Ait-Si-Ali, S., Yokochi, T., Wade, P. A., Jones, P. L. and Wolffe, A. P.** (2000). DNMT1 forms a complex with Rb, E2F1 and HDAC1 and represses transcription from E2F-responsive promoters. *Nat. Genet.* **25**, 338-342.

**Shimada, M., Niida, H., Zineldeen, D. H., Tagami, H., Tanaka, M., Saito, H. and Nakanishi, M.** (2008). Chk1 is a histone H3 threonine 11 kinase that regulates DNA damage-induced transcriptional repression. *Cell* **132**, 221-232.

**Sidman, R. L., Miale, I. L. and Feder, N.** (1959). Cell proliferation and migration in the primitive ependymal zone: an autoradiographic study of histogenesis in the nervous system. *Exp. Neurol.* **1**, 322-333.

**Silva, A. R. T., Santos, A. C. F., Farfel, J. M., Grinberg, L. T., Ferretti, R. E. L., Campos, A. H. J. F. M., Cunha, I. W., Begnami, M. D., Rocha, R. M., Carraro, D. M. et al.** (2014). Repair of oxidative DNA damage, cell-cycle regulation and neuronal death may influence the clinical manifestation of Alzheimer's disease. *PLoS ONE* **9**, e99897.

**Tabata, H. and Nakajima, K.** (2001). Efficient in utero gene transfer system to the developing mouse brain using electroporation: visualization of neuronal migration in the developing cortex. *Neuroscience* **103**, 865-872.

**Tabata, H. and Nakajima, K.** (2003). Multipolar migration: the third mode of radial neuronal migration in the developing cerebral cortex. *J. Neurosci.* **23**, 9996-10001.

**Takai, H., Tominaga, K., Motoyama, N., Minamishima, Y. A., Nagahama, H., Tsukiyama, T., Ikeda, K., Nakayama, K., Nakanishi, M. and Nakayama, K.** (2000). Aberrant cell cycle checkpoint function and early embryonic death in Chk1 (-/-) mice. *Genes Dev.* **14**, 1439-1447.

**Talluri, S. and Dick, F. A.** (2012). Regulation of transcription and chromatin structure by pRB: here, there and everywhere. *Cell Cycle* **11**, 3189-3198.

**Unterberger, A., Andrews, S. D., Weaver, I. C. G. and Szyf, M.** (2006). DNA methyltransferase 1 knockdown activates a replication stress checkpoint. *Mol. Cell. Biol.* **26**, 7575-7586.

**Visel, A., Thaller, C. and Eichele, G.** (2004). GenePaint.org: an atlas of gene expression patterns in the mouse embryo. *Nucleic Acids Res.* **32**, D552-D556.

**Wang, J., Han, X. and Zhang, Y.** (2012). Autoregulatory mechanisms of phosphorylation of checkpoint kinase 1. *Cancer Res.* **72**, 3786-3794.

**Weinberg, R. A.** (1995). The retinoblastoma protein and cell cycle control. *Cell* **81**, 323-330.

**West, M. J., Slomianka, L. and Gundersen, H. J. G.** (1991). Unbiased stereological estimation of the total number of neurons in the subdivisions of the rat hippocampus using the optical fractionator. *Anat. Rec.* **231**, 482-497.

**Xu, X. L., Singh, H. P., Wang, L., Qi, D.-L., Poulos, B. K., Abramson, D. H., Jhanwar, S. C. and Cobrinik, D.** (2014). Rb suppresses human cone-precursor-derived retinoblastoma tumours. *Nature* **514**, 385-388.

**Yang, Y., Geldmacher, D. S. and Herrup, K.** (2001). DNA replication precedes neuronal cell death in Alzheimer's disease. *J. Neurosci.* **21**, 2661-2668.

**Yao, B. and Jin, P.** (2014). Unlocking epigenetic codes in neurogenesis. *Genes Dev.* **28**, 1253-1271.

**Yu, Y., Ren, Q.-G., Zhang, Z.-H., Zhou, K., Yu, Z.-Y., Luo, X. and Wang, W.** (2012). Phospho-Rb mediating cell cycle reentry induces early apoptosis following oxygen-glucose deprivation in rat cortical neurons. *Neurochem. Res.* **37**, 503-511.

**Zhang, J., Gray, J., Wu, L., Leone, G., Rowan, S., Cepko, C. L., Zhu, X., Craft, C. M. and Dyer, M. A.** (2004). Rb regulates proliferation and rod photoreceptor development in the mouse retina. *Nat. Genet.* **36**, 351-360.